

New Phase Modulation Technique Based on Spatial Soliton Switching

Fabio Garzia, Concita Sibilìa, *Member, IEEE, Member, OSA*, and Mario Bertolotti, *Member, OSA*

Abstract—A phase modulation technique able to increase the transmission capacity of an optical channel is presented. It is based on spatial soliton switching properties. The modulator device accepts as inputs two streams of amplitude modulated pulses and generates an output stream of phase modulated pulses whose phase values depends on the different input combinations, coding properly the input streams and increasing the transmission capacity of the optical channel that carries this information. The modulator device can be properly cascaded, generating a unique stream of pulses capable of carrying the information of a certain number of input channels. A proper demodulator device is also presented. It is capable of accepting as input a phase modulated stream of pulses, generating as outputs the original amplitude modulated pulse streams.

Index Terms—All-optical device, optical modulator, spatial solitons, transmission speed increasing.

I. INTRODUCTION

THE DEVICE described in this paper is capable of increasing the transmission capacity of an optical channel. It is based on the special properties of spatial solitons that are, as is well known, self-trapped optical beams able to propagate without any change of their spatial shape, thanks to the equilibrium, in a self-focusing medium, between diffraction and nonlinear refraction [1].

Their interesting properties have allowed design of a certain number of spatial optical switches that utilize the interaction between two bright or dark soliton beams and the waveguide structures induced by these interactions [2]–[6],[19]. Two distinct parallel solitons are generally used as initial condition for such interactions. In fact, it is well known that when two distinct bright spatial solitons are launched parallel to each other, the interaction force between them depends on their relative distance and their phase [7], [8].

A variety of useful devices can be thought of and designed using the properties of solitons. One of the most important features is their particle-like behavior and their relative robustness to external disturbs.

Interesting effects have been found in the study of transverse effects of soliton propagation at the interface between two nonlinear materials [9]–[11] or in a material in the presence of a Gaussian refractive index profile, that is, in low perturbation regime [9].

It has been shown that it is possible to switch a soliton, in the presence of a transverse refractive index variation, toward

a fixed path, because the index variation acts as a perturbation against which the soliton reacts as a particle, moving as a packet without any loss of energy. This last property makes it possible to design useful all-optical devices such as filters [13] or high-speed routers [14].

The general problem of increasing the transmission velocity of an optical channel is felt in the telecommunications field. Here, the general tendency is to compress, as narrowly as possible, the temporal width of pulses using different techniques. This compression can be made until a certain limit, due to the physical limitations of the optical channel used.

The aim of this work is to find a different approach to this problem, supposing to use already compressed binary modulated input pulses as input. We therefore study a device that is able to increase the transmission capacity of an optical channel, extending the modulation also to the phase of output pulses. It acts as an amplitude/phase converter accepting two binary modulated stream of pulses as inputs and generating a unique phase modulated stream of pulses as output. The device can be properly cascaded, generating a unique stream of pulses capable of carrying the information of a certain number of input channels. The great advantage is that the device is totally passive, which means that it does not need extra energy to work properly.

In its basic geometry a soliton beam travels in a waveguide, which, in the plane between the cladding and the substrate, has a distribution of refractive index that follows a triangular curve with a modified parabolic profile as shown in Fig. 1.

We begin studying the general structure of the device. Then, the transverse behavior of a soliton in a triangular profile [13], whose longitudinal profile is parabolic [14], is discussed. Once the properties of motion are derived, we investigate the structure from the global point of view, deriving all the properties and the operative conditions. Last, we discuss a proposal for the demodulator.

II. STRUCTURE OF THE MODULATOR DEVICE

To simplify the development of the theory, we consider only a two-input/one-output device. The purpose of the modulator device is to generate a phase modulated pulse according to the different combinations of amplitude of input pulses. This is equal to saying that in the presence of two binary inputs, the possible amplitude combinations are four, and the output pulse has to assume four different phase values, without requesting auxiliary energy. Because we want to design a passive device, the output related to the situation of both inputs equal to zero must obviously be codified with an absence of pulse. The schematic pattern of input–output conversion is shown in Fig. 1(a).

Manuscript received March 17, 2000; revised March 9, 2001.

The authors are with the Dipartimento di Energetica, INFM, Università di Roma “La Sapienza,” 00161 Roma, Italy.

Publisher Item Identifier S 0733-8724(01)05302-6.

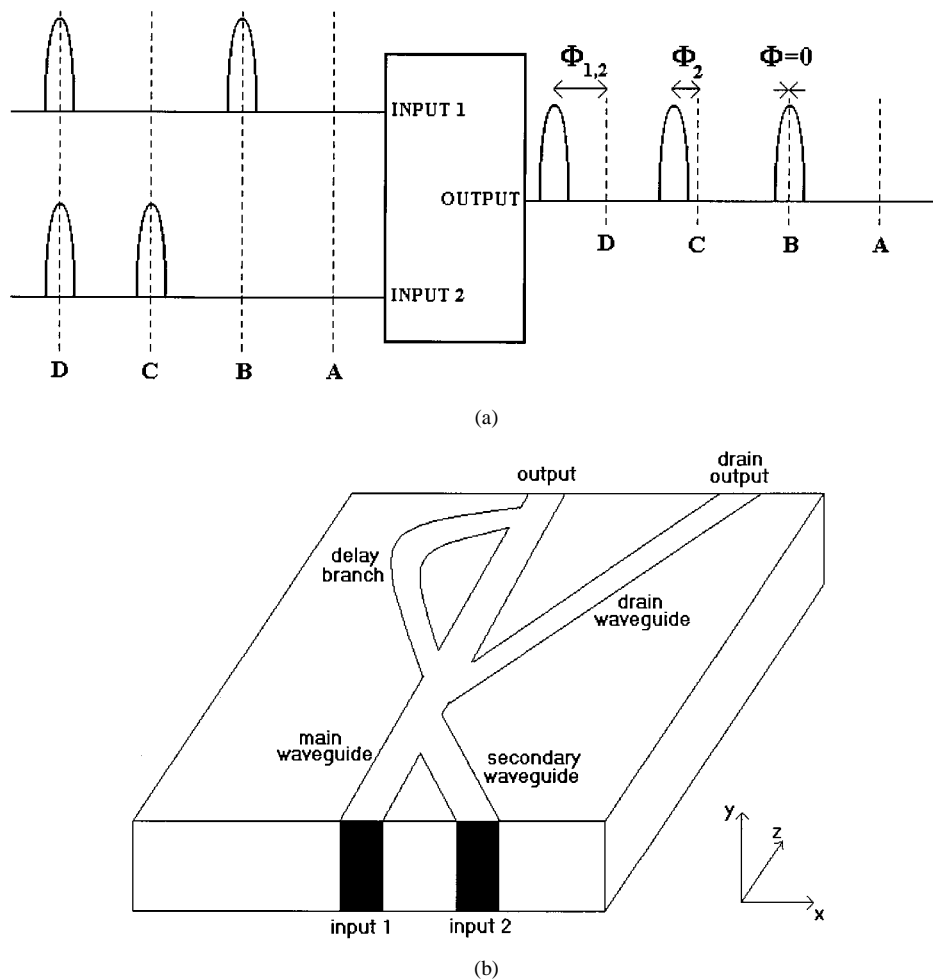


Fig. 1. (a) Schematic pattern of input–output pulse conversion. (b) Three-dimensional (3-D) view of the structure of the considered device.

We suppose to work with soliton beams to use their attracting or repelling properties [7] and their particular behavior when they propagate in a transverse refractive index profile [13]. The structure we want to study is shown in Fig. 1(b).

We also suppose that the two input pulses enter in the relative inputs of the device with the same phase. This is not a restriction because any phase difference can be properly compensated.

Owing to the fact that we deal with equal streams of pulses, the last condition is that the input pulses are characterized by the same amplitude.

The modulator device is composed of four parts: the main waveguide, the secondary waveguide, the delay branch, and the drain waveguide. The geometry and the refractive index values of these four components strictly determine the feature of the device, and their values will be designed as discussed in the following.

Let us analyze the behavior of the modulator device in the four possible input situations. Because we deal with binary input pulses, we consider the two values of logical zero (absence of pulse) and logical one (presence of pulse). We refer to them as zero and one.

The first situation is when the two inputs are equal to zero. In this case, due to the passive nature of the device, we obtain a zero in the output.

The second situation is when the first input is equal to one and the second input is equal to zero. In this case, if the refractive index of both the delay branch and the drain waveguide is less than or equal to the refractive index of the main waveguide, the pulse propagates undisturbed and reaches the output, with a phase that is equal to the propagation phase along the main waveguide. If the length of this waveguide is properly chosen, according to the wavelength of the beam, the phase of the output pulse is equal to the phase of the input pulse. In the first situation, there was an absence of pulse and its phase value was virtually equal to zero. In this case, the phase value variation has been chosen equal to zero, but we are in the presence of a pulse. The phase variation could anyway be chosen at will, but we keep it fixed at zero for simplicity. The behavior of this kind of waveguide has already been studied [13].

The third situation is when the first input is equal to zero and the second input is equal to one. In this case, because we are in the proper refractive index conditions of the waveguide and the delay branch is properly shifted with respect to the input point of the secondary wave, the second input pulse is trapped in the main waveguide and reaches the output with a certain phase difference that we define later, with respect to the previous case, due to the fact that it propagates, in the initial part, into the secondary waveguide.

TABLE I
WORKING SCHEME OF THE DEVICE

N°.	INPUT 1 (INTENSITY)	INPUT 2 (INTENSITY)	OUTPUT INTENSITY	OUTPUT PHASE	PHASE CONDITION
1	0	0	0	0	-
2	I_1	0	I_1	0	-
3	0	I_2	I_2	φ_2	$\frac{\pi}{2} < \varphi_2 < \frac{3\pi}{2}$
4	I_1	I_2	I_1	$\varphi_{1,2}$	-

The fourth situation is when both the inputs are equal to one. In this case, the two pulses meet at the converging point between the main waveguide and the secondary waveguide. In this case, since we are in soliton propagation condition, they can attract if their relative phase is included between zero and $\pi/2$ or between $3\pi/2$ and 2π , or they can repel if their relative phase is included between $\pi/2$ and $3\pi/2$. If the length of the secondary waveguide is chosen to generate a repulsive condition, the two solitons propagate in the main waveguide properly separated until reaching the bifurcation point between the main waveguide, the delay branch, and the drain waveguide. At this point, the two solitons detach: the first one enters the delay branch while the second one enters the drain waveguide.

The first soliton propagates in the delay branch, experiencing a phase variation that depends on the length of the branch and therefore is properly selectable and can be chosen different from the previous cases, generating the fourth phase condition. The second pulse, on the contrary, propagates in the drain waveguide where it reaches the proper drain output.

The delay branch is composed by a properly modified longitudinal parabolic waveguide, whose purpose is to accept the beam from the main waveguide with an angle that respects the paraxial approximation, to propagate it changing its direction until reaching a straight longitudinal direction, and to reverse this sequence until carrying the pulse inside the main waveguide with a certain phase difference. The behavior of this modified parabolic waveguide is studied later.

The situation is summarized in Table I, where it is also pointed out that the pulse reaches the output to provide more details about the working principles of the modulator device, even if we consider input pulses with the same amplitude.

We will now better define the profile of the refractive index of the waveguides and the properties of the longitudinal modified parabolic waveguide that compose the delay branch.

III. PROPERTIES OF A SOLITON IN A MODIFIED LONGITUDINAL PARABOLIC WAVEGUIDE

We now define the structure of the modified parabolic waveguide composing the delay branch to find its peculiar properties that allow the loop to work properly.

We choose this kind of waveguide because it is the simplest curve that carries progressively the soliton beam from a propagation angle that respects the paraxial approximation until an angle that respects a parallel longitudinal propagation, and vice versa.

This curve could be roughly approximated with a linear curve, but the final result would be too sharp a path, since the soliton reaches the reversing point with a certain inclination. Further, the parabolic path is the trajectory followed from a soliton beam that is injected into a linear transverse refractive index profile, that is, the transverse profile that we are going to consider.

Let us consider a soliton beam propagating in the z -direction, whose expression of the field Q at the beginning of the structure is

$$Q(x, 0) = C \operatorname{sech}[C(x - \bar{x})] \quad (1)$$

where \bar{x} is the position of the center of the beam and C is a real constant from which both the width and the amplitude of the field depend. The variables x and z are normalized with respect to the wave vector of the wave, and therefore they are adimensional quantities.

When the soliton beam is propagating in a triangular transverse index profile, whose maximum value is Δn_0 and whose maximum width is $2b$, it is subjected to a transverse acceleration equal to [13]–[16]

$$a_T = \frac{2\Delta n_0}{b} C^2. \quad (2)$$

We use, for our analysis, a dynamic point of view to consider the step-by-step transverse relative position of the waveguide with respect to the beam using the z -variable as a time parameter.

If $x_G(z)$ is the position of the central part of the waveguide profile with respect to z , the longitudinal form of the waveguide is chosen to be a modified parabolic

$$x_G(z) = \frac{z^2}{a^2} - \frac{2\sqrt{d}}{a} z \quad (3)$$

where a is a real constant responsible for the curvature of the waveguide and d is a real constant responsible for the position of the curve. Equation (3) can be better understood if it is expressed as a function of z , that is

$$z = -a\sqrt{x_G + d} + a\sqrt{d}. \quad (4)$$

It is possible to see that it is positioned in the second quadrant of the Cartesian plane and has a vertical asymptote at $x_G(z) = d$ when $z \rightarrow a\sqrt{d}$. It shows a gradually increasing derivative, growing from a starting angle at $x = 0$, chosen to be below

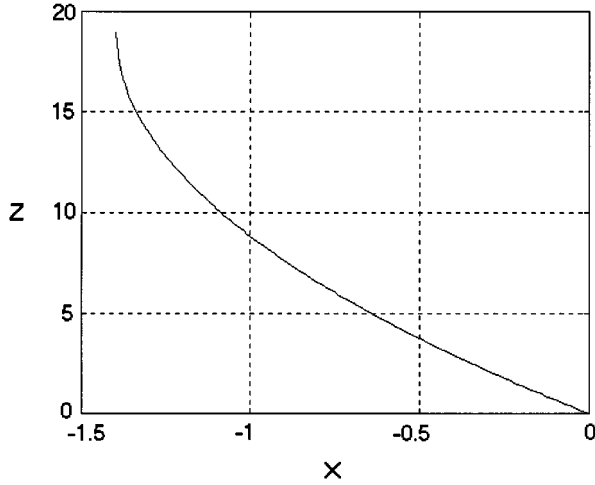


Fig. 2. Graphical representation of the modified parabolic waveguide for $a = 16.9$, $d = 1.4$.

the maximum angle allowed from the paraxial approximation, until reaching a vertical alignment at $x_G(z) = d$; that is what we want to make the device work properly. To respect this term, it is necessary to impose a certain condition to the a and d parameters, as we show later. A graphical representation of (4) is shown in Fig. 2 for $a = 16.9$ and $d = 1.4$.

The local inclination of the waveguide with respect to the longitudinal axis z can be regarded as the transverse relative velocity of the waveguide that appears to the beam that propagates longitudinally

$$v_G = \frac{dx_G(z)}{dz} = \frac{2z}{a^2} - \frac{2\sqrt{d}}{a}. \quad (5)$$

Using (2), it is possible to calculate the transverse relative velocity

$$v_B = \int_0^z a_T d\zeta = \frac{2\Delta n_0}{b} C^2 z \quad (6)$$

and the position of the beam

$$x_B = \int_0^z v_B d\zeta = \frac{\Delta n_0}{b} C^2 z^2. \quad (7)$$

Equation (7) is valid for a propagation in the first quadrant of Cartesian plane. Because we consider, in our case, a propagation in the second quadrant, we must reverse the sign of the second member of the equation considered.

Initially, the beam is positioned in the center of the waveguide. Because the waveguide appears to move with respect to an observer that follows the longitudinal direction, with a relative velocity expressed by (5), the soliton beam enters in the constant acceleration zone, where its velocity increases linearly with z . It also follows a parabolic trajectory, according to (7), until it remains in this part of the waveguide.

After the beam has propagated for a certain z distance, two different situations may occur: the beam leaves the acceleration zone without reaching the velocity of the waveguide at that z or the beam acquires a velocity that is greater than or equal to the

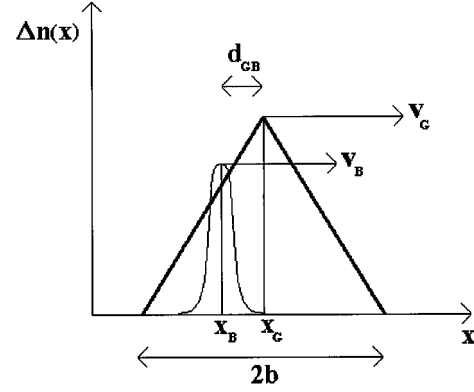


Fig. 3. Relative distance waveguide soliton at some propagation distance z .

velocity of the waveguide. The first event may be called “detach situation,” since the beam leaves the waveguide, while the second one may be called “lock-in situation,” because the beam reaches the other side of the waveguide where it is stopped, reversing its path and so on. At any value of z , as shown in Fig. 3, the distance d_{BG} between the beam and the waveguide is

$$\begin{aligned} d_{BG} &= x_B - x_G = -\frac{\Delta n_0 C^2}{b} z^2 - \frac{z^2}{a^2} + \frac{2\sqrt{d}}{a} z \\ &= -z^2 \left(\frac{b - a^2 \Delta n_0 C^2}{a^2 b} \right) + \frac{2\sqrt{d}}{a} z. \end{aligned} \quad (8)$$

A detach situation takes place when

$$d_{BG} = b. \quad (9)$$

If we solve (9) with respect to z , we can calculate, if it exists, the propagation distance where the detachment begins

$$z_D = \frac{\sqrt{d} \pm \sqrt{d - b - a^2 \Delta n_0 C^2}}{\frac{b + a^2 \Delta n_0 C^2}{ab}}. \quad (10)$$

The two solutions refer to the detach situation (when the negative sign of the root is considered) or to the first cross of the center of the waveguide in the lock-in situation (when the positive sign of the root is considered). Studying the discriminator of (10), it is possible to derive the value of the amplitude C_D that divides the lock-in values from the detach values

$$C_D = \frac{1}{a} \left(\frac{d - b}{\Delta n_0} \right)^{1/2}. \quad (11)$$

It is possible to see from (11) that the more the curvature of the waveguide (a parameter) increases or the more the refractive index decreases, the more C_D increases. This behavior agrees with what one could expect.

We want now to calculate the inclination according to which a soliton, whose amplitude is smaller than the detach amplitude, leaves the waveguide. Since the mentioned angle is equal to the detach velocity, substituting (11) into (6), we have

$$\Phi = \tan^{-1} v_D \quad (12a)$$

$$\begin{aligned} v_D &= v_B(z_D) \\ &= \frac{2\Delta n_0 C^2 a}{b + a^2 \Delta n_0 C^2} (\sqrt{d} - \sqrt{d - b - a^2 \Delta n_0 C^2}). \end{aligned} \quad (12b)$$

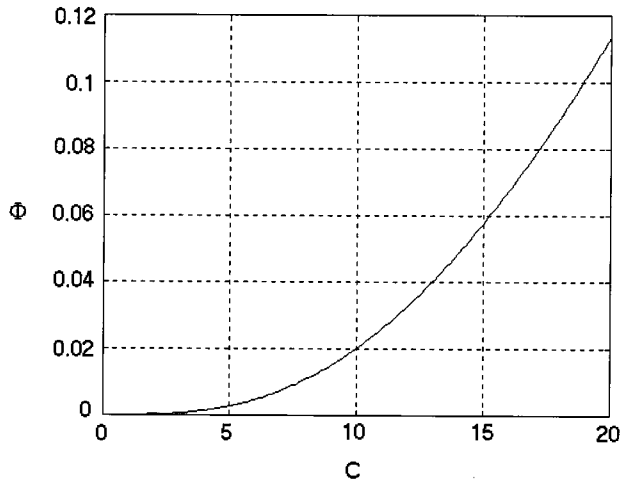


Fig. 4. Detach angle Φ in degrees, equal to $\text{atan}(v_D)$, versus C for $a = 16.9$, $d = 1.4$, $b = 0.25$, $\Delta n_0 = 1.10^{-5}$.

In Fig. 4, it is shown that the graphical behavior of (12) for $a = 16.9$, $d = 1.4$, $b = 0.25$, $\Delta n_0 = 1 \cdot 10^{-5}$. The detach value C_D can be calculated by means of (11) and is equal to 20.

Due to the absence of restrictions about the length L of the waveguide, the lock-in value C_D of the amplitude, expressed from (11), does not depend on L . This means that given a certain waveguide whose length is equal to L , we can obtain a lock-in value C_D whose detachment distance, calculated from (10), is longer than L . In this situation, due to the restriction imposed from the waveguide length L , the detach value C_D obviously decreases. In fact, even if the beams characterized from an amplitude less than C_D tend to be expelled from the waveguide, the detachment takes place at a distance that is longer than the waveguide length L and the beam remains locked in. The new value C_{DL} , which is lower than C_D , can be calculated from (10) setting $z_D = L$ and solving with respect to C

$$C_{DL} = \sqrt{\frac{-B + \sqrt{B^2 - 4AC}}{2A}} \quad (13)$$

where

$$A = a^4 \Delta n_0^2 L^2 \quad (13a)$$

$$B = 2a^2 b L^2 \Delta n_0 - 2a^3 b \sqrt{d} L \Delta n_0 + a^4 b^2 \Delta n_0 \quad (13b)$$

$$C = b^2 L^2 - 2ab^2 L \sqrt{d} + a^2 b^3. \quad (13c)$$

We want now to make some considerations about the paraxial approximation.

Because we deal with a modified parabolic waveguide, we are in the presence of a curvature, with respect to the z axis, that increases with z . We cannot forget that we are in a paraxial approximation, that is, the derived equations are valid until the angle between the propagation direction and the longitudinal direction is less than $8^\circ \div 10^\circ$. This means that due to the analytical expression of the waveguide, expressed by (3) or (4), once the a or d parameter has been chosen, the other parameter is unavoidably fixed. The condition must be imposed only at the entrance of the waveguide, where the curvature, with respect to

the longitudinal direction, is maximum and decreases up to zero at the end. In analytical terms, this means that it is possible to impose this condition to the first derivative of (3) to calculate the maximum propagation distance

$$|x'_G(0)| = \frac{2\sqrt{d}}{a} \leq \tan 8^\circ = 0.14 \quad (14)$$

that gives

$$\frac{\sqrt{d}}{a} \leq 7.10^{-2}. \quad (15)$$

This condition must be considered in the project of the delay branch.

We want now to calculate the length of the curve expressed by (3), since it is necessary to control the optical path, and therefore the phase variation, of the beam that propagates inside it.

Considering (4), the first derivative of z with respect to x is

$$\frac{dz}{dx} = -\frac{a}{2\sqrt{x+d}} \quad (16)$$

and the elementary length of the curve, as a function of x , is

$$dl = \sqrt{dx^2 + dz^2} = \sqrt{dx^2 + \frac{a^2}{4(x+d)} dx^2}. \quad (17)$$

Integrating (17), we have

$$I(x) = \frac{(x+d)\sqrt{\frac{4x+4d+a^2}{x+d}}}{2} + \frac{a^2}{8} \log \left(8x + 8d + a^2 + 4(x+d) \cdot \sqrt{\frac{4x+4d+a^2}{x+d}} \right) + \text{constant}. \quad (18)$$

It is possible to see that the integral becomes indefinite when x tends to $-d$, as one could expect due to the structure of the curve. To define the constant that is present in (18), it is necessary to calculate the limit of the integral when x tends to $-d$

$$\lim_{x \rightarrow -d} I(x) = \frac{a^2}{4} \log a. \quad (19)$$

The length of the curve is therefore equal to

$$\begin{aligned} L_G &= I(0) \\ &= \frac{d}{2} \sqrt{\frac{4d+a^2}{d}} + \frac{a^2}{8} \log \left(8d + a^2 + 4d \sqrt{\frac{4d+a^2}{d}} \right) \\ &\quad - \frac{a^2}{4} \log a \end{aligned} \quad (20)$$

that is obviously a complex function of a and d parameters.

IV. NUMERICAL SIMULATION OF THE MODULATOR DEVICE

We have simulated the modulator device from the numerical point of view using a finite difference beam-propagation method

(FD-BPM) algorithm to study its behavior and to see if it agrees with the developed theory.

At first, the design does not consider the physical limitations that can arise when we deal with technological fabrication problems. Next, we will consider this kind of problem.

We use a geometrical approach in this situation, that is, we do not care of imposing particular conditions that would be necessary in a real situation, such as to use the same Δn_0 for all the waveguides, letting us use a higher number of degrees of freedom. We are further free of using the wavelength we need to generate the proper phase variation according to our needs. This is obviously not possible in a real case where the wavelength is given.

Let us choose, for example, the half-length of the delay branch waveguide equal to 20

$$a\sqrt{d} = 20. \quad (21)$$

Since we have to respect, even in this design approach, the paraxial condition, we have to solve the system of equations composed by (21) and (15) that gives $a = 16.9, d = 1.4$.

The width of the waveguide must obviously be less than d , and we choose, for example, $b = 0.25$, supposing a waveguide width equal to $2b = 0.5$.

The spot size of the beam must be less than or equal to b . Since we deal with a hyperbolic secant profile, expressed by (1), the width is linked to the amplitude C . That is, the greater C is, the narrower the beam. A proper value is $C = 20$. The difference of length between the interested part of the main waveguide and the delay branch can be calculated using (20), which gives $\Delta L_G = 0.1305$. Once the wave vector is chosen, we immediately have the phase difference.

We have not, until this point, chosen the phase values to code. We decide to generate a phase difference a bit greater than $\pi/2$ for the passage through the secondary waveguide and a phase difference a greater than π for the passage through the delay branch. This is equal to saying that the length of the delay branch must almost be twice the length of the secondary waveguide. Since the length of the delay branch has already been chosen, we have to design the secondary waveguide. A proper structure is, for example, the one whose projections on the longitudinal and transversal directions are, respectively, equal to 35 and 2. That gives a difference of length between the interested part of the main waveguide and the secondary waveguide equal to 0.0571, which is less than one-half of the relative difference of length of the delay branch.

We now must find the value of the wave vector that allows us to obtain the chosen phase values. A good value is $\beta = 30$, which gives a phase value of 1.24π for the delay branch and a phase value of 0.55π (a bit larger than the minimum value of $\pi/2$ that allows the repulsion between two close soliton beams) for the secondary waveguide.

Once all the geometrical values of the structure are chosen, it is necessary to select the refractive index of the waveguides to ensure the correct trapping of the beams inside them.

From (11), we have

$$\Delta n_{0G} = \frac{d-b}{a^2 C_D^2}. \quad (22)$$

Substituting the numerical values, we have $\Delta n_{0G} = 1 \cdot 10^{-5}$.

Since for the secondary waveguide we have [13]

$$C_D = \frac{V_G}{2(\Delta n_{0S})^{\frac{1}{2}}} \quad (23)$$

where v_G is the tangent of the angle between the waveguide and the longitudinal direction, it is possible to solve (23) with respect to Δn_{0S} , giving

$$\Delta n_{0S} = \left(\frac{V_G}{2C_D} \right)^{\frac{1}{2}}. \quad (24)$$

Substituting the numerical values, we have $\Delta n_{0S} = 2.04 \cdot 10^{-6}$, which is five times less than the value found for the delay branch. This difference reflects the different geometry, and therefore the different propagation conditions, of the two considered optical structures. We further choose for the main waveguide a refractive index value equal to $\Delta n_{0G} = 1 \cdot 10^{-5}$, so that the beam that propagates inside the main waveguide does not enter in the delay branch unless it is pushed inside it.

The design approach used until this point is obviously practical for the numerical simulations because, as we already said, we have no physical restrictions. However, it is impossible to use it in a real device design due to the greater number of limitations. We show a real design approach in the following.

Further, we neglect to insert at the end of the structure a proper propagation distance that allows the beam that enters alone in the structure through input 1 to exit with the same input phase, since we are mainly interested to the phase variations. The drain waveguide has been designed similar to the secondary waveguide.

The geometry of the designed structure is shown in Fig. 5(a). Let us analyze the results of the numerical simulations for the three possible input combinations to demonstrate the correctness of the developed theory, neglecting the situation of no inputs that represents the first combination according to Table I.

In Fig. 5(b), the numerical simulation in the case of the presence of the only input pulse at entrance 1 (the second input combination of Table I) is shown. In this case, since the refractive index variation is equal to that of the delay branch, the beam propagates undisturbed and reaches the output, generating a proper phase coded pulse.

In Fig. 5(c), the numerical simulation of the third input combination, which is the presence of only an input pulse at entrance 2, is shown. In this case, the pulse first propagates properly trapped inside the secondary waveguide, due to the fact that the parameters of the structures have been designed to lock it. It reaches the main waveguide with a certain phase difference that we have designed to be equal to 0.55π , reaching the output and generating a proper output phase coded pulse.

In Fig. 5(d), the numerical simulation of the fourth input combination, which is the presence of both input pulses at the entrances, is shown. In this case, the two pulses meet at the merging point between the main waveguide and the secondary waveguide with a relative phase difference greater than 0.55π , which is in a repulsive situation. The two beams propagate parallel each other properly separated until reaching the bifurcation point. In this zone, the pulse relative to input 1

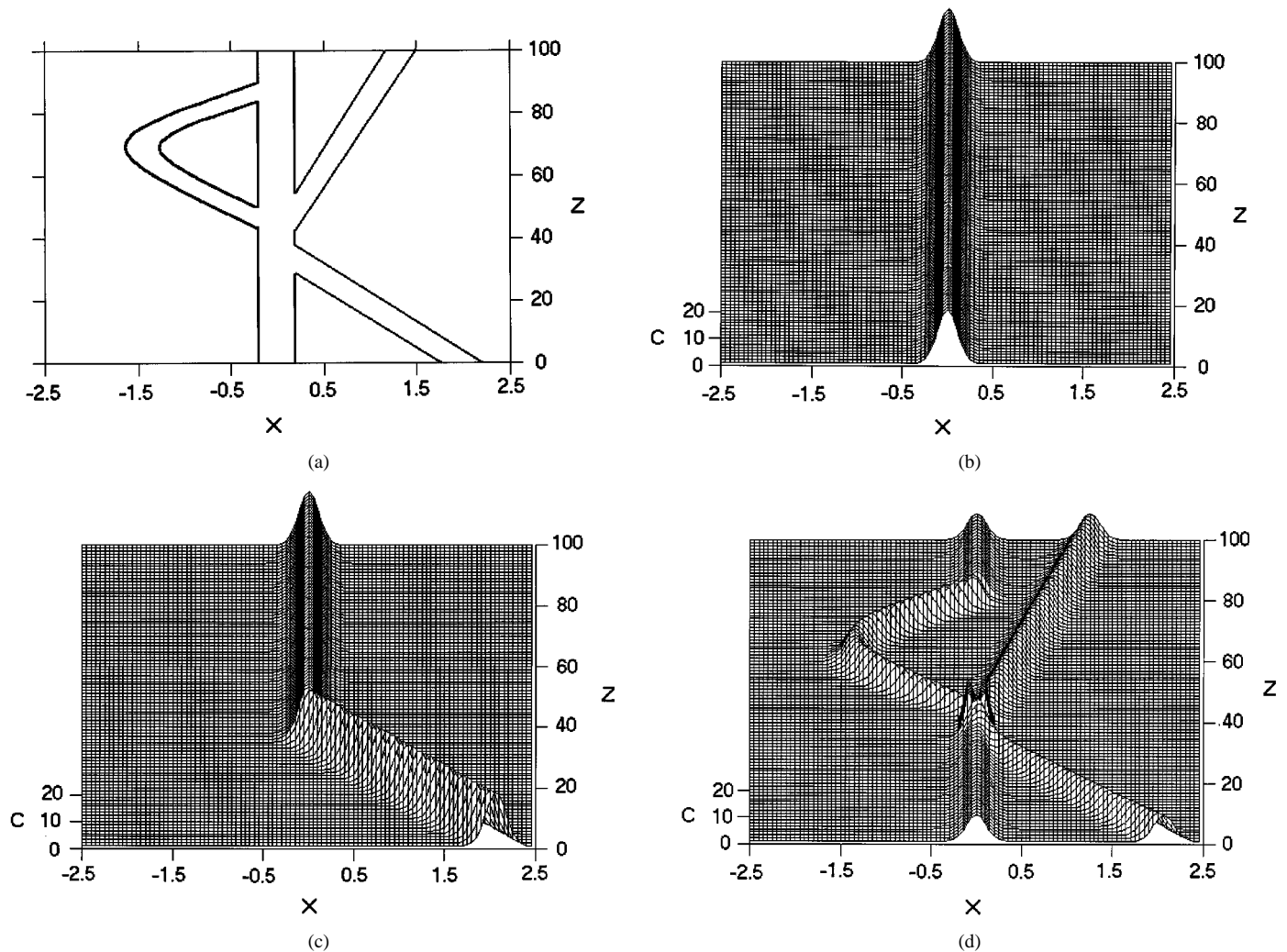


Fig. 5. Upper view and numerical simulations. The parameters of the waveguide are $a = 16.9$, $d = 1.4$, $b = 0.25$, $\Delta n_0 = 1 \cdot 10^{-5}$. (a) Upper view of the structure. Numerical simulation of the behavior of the structure in the presence of (b) only input 1, (c) only input 2, and (d) both input 1 and input 2.

is pushed into the delay branch, while the pulse relative to input two is pushed inside the drain waveguide where it reaches the drain output. The first pulse, which propagates inside the delay branch, is trapped inside it since the structure has been properly designed, and enters again inside the main waveguide with a relative designed phase difference equal to 1.24π , reaching the output and generating a proper output phase coded pulse.

The numerical simulations, as shown in Fig. 5, confirm the theory developed.

V. NUMERICAL DESIGN OF A PRACTICAL MODULATOR DEVICE

We now give a numerical example for a practical design of the considered modulator device.

We suppose having a Schott B 270 glass, whose optical parameters at $\lambda_0 = 620$ nm are $n_0 = 1.53$ and $n_2 = 3.4 \cdot 10^{-20} \text{ m}^2/\text{W}$, with n_0 and n_2 being the linear and nonlinear refractive indexes, respectively [13]. Let us consider a spot size of the beam equal to $d_0 = 10 \mu\text{m}$.

The design rules are very restrictive in a real situation since it is necessary to match different requests with a reduced free choice of parameters. In fact, once the source and the proper material for the given source are fixed, it is necessary to design the

geometry of the structure to trap the pulses with a proper soliton intensity level, generating the necessary coded phase variation. Further, since we use the same constructive technology, we suppose that the refractive index variation Δn_0 is the same for the delay branch and for the secondary waveguide, introducing another restriction.

It is well known that given a certain material and a certain light source, the intensity necessary to generate a soliton beam is given by

$$I_s = \frac{2n_0}{d_0^2 n_2 \beta^2} \quad (25)$$

where β is the wave vector of the beam. Substituting the numerical values into (17), we have $I_s = 3.74 \cdot 10^{15} \text{ W/m}^2$.

Since the intensity of the beam I_s is related to its amplitude C from [13]

$$I_s = \frac{1}{[\log(2 + \sqrt{3})]^2} \frac{n_0}{2n_2} C^2 \quad (26)$$

it is possible to express (11) and (23) in terms of the intensity of the beams.

We choose, for example, $\Delta n_0 = 1 \cdot 10^{-2}$, and we start with the design of the device. We want to code the third situation (only a pulse at the input 2) with a relative phase variation just greater than $\pi/2$ and the fourth situation (both the input pulses) with a relative phase very close to π .

We choose $d = 2d_0 = 20 \mu\text{m}$. Substituting this value into (15), we obtain $a = 0.0639$. In this way, the geometry of the delay branch is totally defined. If we choose $b = 19.96 \mu\text{m}$, using (11) and (26), we obtain a lock-in value $I_D = 1.25 \cdot 10^{16} \text{W/m}^2$, that is, a value above the soliton threshold calculated with (25) and below the second-order soliton threshold.

We now must to check if, with these values, we have obtained a phase difference value very close to π , as we desire. The phase difference value can be calculated as the product of the wavevector and the difference of path between the delay branch and the main waveguide. Using (20), we obtain $\Delta\phi = 0.59\pi$. This value is very close to the other phase value, generating two phase values very close each other. In this case, it is necessary to make some correction to the geometry of the delay branch to correct the phase value to a value close to π , keeping at the same time the lock intensity above the soliton generation threshold. We choose to increase the value of the “ a ” parameter, which allows the paraxial approximation to be conserved. If we increase this parameter by 1.53 times, the total length of the delay branch increases. The new intensity lock-in value decreases to $I_D = 5.36 \cdot 10^{15} \text{W/m}^2$, which is always above the soliton generation threshold. The phase value is in this case equal to π , as we desired at the beginning of our computation.

It is now necessary to project the secondary input waveguide. We want to obtain the same intensity lock-in value calculated for the delay branch and a phase difference value a bit greater than $\pi/2$.

This kind of waveguide has already been studied [13], showing a behavior similar to the parabolic waveguide and a lock-in value equal to

$$C_D = \frac{v_G}{2(\Delta n_0)^{\frac{1}{2}}} \quad (27)$$

where v_G is the tangent of the inclination angle with respect to the longitudinal direction. It is obviously necessary to respect, even in this case, the paraxial approximation; this means that once we have chosen the distance a_L between the second input and the main input, the longitudinal length b_L of the waveguide cannot be shorter than a minimum, calculated according to the paraxial limit, that is

$$a_L \leq b_L \tan 8^\circ = 0.14b_L. \quad (28)$$

Since we suppose to generate this waveguide using the same physical procedure used for the delay branch, we have to suppose that the value $\Delta n_0 = 1 \cdot 10^{-2}$ is the same for both waveguides. If we use as a first attempt value $a_L = d$ to generate a device whose lateral extensions with respect to the main waveguide are the same, we immediately obtain b_L from (28), which allows us to calculate v_G . Substituting these values into (27), using (26), we have an intensity lock-in value equal to $I_{DS} = 2.23 \cdot 10^{17} \text{W/m}^2$ and $\Delta\phi_S = 1.12\pi$. The waveguide

designed according to these criteria is totally useless for our purpose since the lock-in value is greatly above the generation value of a second-order soliton and consequently above the lock-in value calculated for the delay branch. Further, the phase value obtained is totally different with respect to the one we desire. It is therefore necessary to find another approach. If we impose the waveguide to have the same lock-in intensity of the delay branch, considering always $a_L = d$, we can calculate b_L , reversing the reasoning followed above. In this case, we obtain $b_L = 5650 \mu\text{m}$, which satisfies the paraxial condition expressed by (27). If we calculate the phase difference, we have $\Delta\phi_S = 0.175\pi$, which is not only a different value respect to the desired one but also a value that does not allow the repulsion between the two beams, a fundamental condition to make the device to operate correctly.

Consequently, it is necessary to act also on a_L , considering a device that does not have the same lateral extension with respect to the main waveguide. Fixing the intensity lock-in level to be equal to that of the delay branch and fixing the phase difference $\Delta\phi_S$ to be as close as possible to 0.5π , it is possible to demonstrate that a valid waveguide is the one characterized by $a_L = 3d = 60 \mu\text{m}$ and $b_L = 16935 \mu\text{m}$ and that provides a phase difference $\Delta\phi_S = 0.53\pi$, respecting the paraxial condition expressed by (27).

The problems found in the design of the secondary input waveguide could be avoided if we could act also on Δn_0 , but this is very difficult to achieve in a real situation, where both the delay branch and the inclined waveguide are generated in the same process.

Different approaches can be used to design the modulator device, as, for example, to dimension first the secondary waveguide and the delay branch, but they are always subjected to different restrictions due to the physics of the waveguide generation process.

VI. DEVICE CASCADING

We now study the possibility of cascading N different modulator devices to generate a unique device capable of increasing the transmission velocity by $2N$ times.

We first study the situation of a cascade of two modulator devices, as shown in Fig. 6. In this case, we have two input devices, first-level devices with two inputs each, for a total of four inputs named I_1, I_2 for the first device and I_3, I_4 for the second device. The devices generate two double-speed output flows that enter a third, second-level device, with two inputs named I_A, I_B to distinguish them from the inputs of the first-level devices. The working schemes of the second and third devices are, respectively, shown in Tables II and III. It is necessary to note that the phase conditions imposed for the first-level devices are not valid, at the moment, for the second-level device, since this device works on already phase modulated pulses. Its phase conditions will be derived in the following.

We will alternatively use, in the following, the definition of first-level devices for the first and second devices. Analogously, we use the definition of second-level device for the third device.

We want now to combine Tables I–III to find the phase conditions that allow the cascade to work properly. This means that

TABLE II
WORKING SCHEME OF THE SECOND DEVICE (FIRST-LEVEL DEVICE)

N°.	INPUT 3 (INTENSITY)	INPUT 4 (INTENSITY)	OUTPUT INTENSITY	OUTPUT PHASE	PHASE CONDITION
1	0	0	0	0	-
2	I_3	0	I_3	0	-
3	0	I_4	I_4	φ_4	$\frac{\pi}{2} < \varphi_4 < \frac{3\pi}{2}$
4	I_3	I_4	I_3	$\varphi_{3,4}$	-

TABLE III
WORKING SCHEME OF THE THIRD DEVICE (SECOND-LEVEL DEVICE). THE PHASE CONDITIONS ARE NOT PRESENT HERE SINCE THEY ARE DERIVED FROM THE CONDITIONS IMPOSED FROM THE CASCADE CONNECTION

N°.	INPUT A (INTENSITY)	INPUT B (INTENSITY)	OUTPUT INTENSITY	OUTPUT PHASE	PHASE CONDITION
1	0	0	0	0	-
2	I_A	0	I_A	0	-
3	0	I_B	I_B	φ_B	-
4	I_A	I_B	I_A	$\varphi_{1,2}$	-

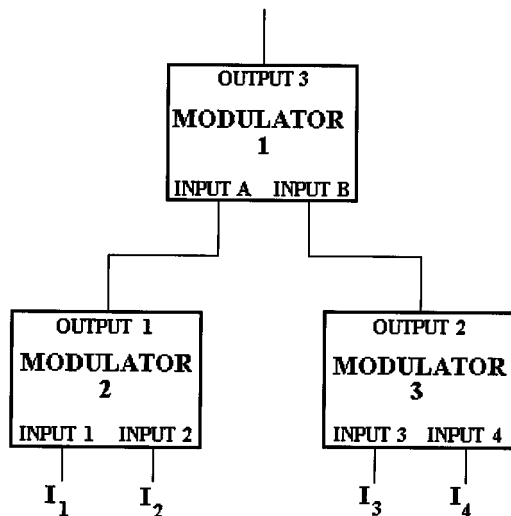


Fig. 6. Cascade of 2+1 devices.

it is necessary to analyze all the possible input combinations to see if the phase conditions imposed from the first-level devices match with the phase conditions imposed from the second-level device.

We will indicate in the following a pulse whose amplitude is I and whose phase is φ with the notation $I|\varphi$.

The working scheme of the cascade, which we are going to discuss in detail, is shown in Table IV.

The first four input situations are rather clear since they do not require the action of the second-level device and the output pulses conserve the phase modulation of the first device.

Situation 5 is when there is only one pulse at input 3. In the case of the pulse exit of the second device with no phase modulation, according to Table II and using Table III, we see

that the pulse is only phase modulated from the second-level device without experiencing any interaction with other pulses. This does not yet allow us to impose any phase condition on situation 3 of Table III.

Situation 6 is quite complex since it implies an interaction inside the second-level device. In this case, a pulse $I_1|0$ exits the first device and enters the input A second-level device, while a pulse $I_3|0$ exits the second device and enters the input B second-level device, where it propagates in the secondary input waveguides, emerging as $I_3|\varphi_B$. The two pulses meet at a converging point between the delay branch and the secondary input waveguide of the second-level device. Since it is necessary for the two pulses to repel each other, we obtain

$$\frac{\pi}{2} < \varphi_B < \frac{3\pi}{2} \quad (29)$$

as the phase condition for the third device that completes the phase condition of Table III. Due to this repulsive action, we obtain $I_1|\varphi_{A,B}$ as final output.

Situation 7 is represented from a pulse $I_2|\varphi_2$ that exits the first device and enters the input A second-level device, while a pulse $I_3|0$ exits the second device and enters the input B second-level device, where it propagates in the secondary input waveguides, emerging as $I_3|\varphi_B$. The repulsion takes place if

$$\frac{\pi}{2} < \varphi_B - \varphi_2 < \frac{3\pi}{2} \quad (30)$$

that generates $I_2|\varphi_2 + \varphi_{A,B}$ as output. To respect this phase condition, it is necessary to make further restrictions on φ_2 and φ_B that are

$$\frac{\pi}{2} < \varphi_2 < \pi \quad (31)$$

$$\pi < \varphi_B < \frac{3}{2}\pi. \quad (32)$$

TABLE IV
WORKING SCHEME OF THE CASCADE DEVICE

N°.	INPUT 1 (INTENSITY)	INPUT 2 (INTENSITY)	INPUT 3 (INTENSITY)	INPUT 4 (INTENSITY)	OUTPUT INTENSITY	OUTPUT PHASE	PHASE CONDITION
1	0	0	0	0	0	0	-
2	I_1	0	0	0	I_1	0	-
3	0	I_2	0	0	I_2	φ_2	-
4	I_1	I_2	0	0	I_1	$\varphi_{1,2}$	-
5	0	0	I_3	0	I_3	φ_B	-
6	I_1	0	I_3	0	I_1	$\varphi_{A,B}$	$\frac{\pi}{2} < \varphi_B < \frac{3\pi}{2}$
7	0	I_2	I_3	0	I_2	$\varphi_2 + \varphi_{A,B}$	$\frac{\pi}{2} < \varphi_B - \varphi_2 < \frac{3\pi}{2}$
8	I_1	I_2	I_3	0	I_1	$\varphi_{1,2} + \varphi_{A,B}$	$\frac{\pi}{2} < \varphi_B - \varphi_{1,2} < \frac{3\pi}{2}$
9	0	0	0	I_4	I_4	$\varphi_4 + \varphi_{A,B}$	-
10	I_1	0	0	I_4	I_1	$\varphi_{A,B}$	$\frac{\pi}{2} < \varphi_4 + \varphi_B < \frac{3\pi}{2}$
11	0	I_2	0	I_4	I_2	$\varphi_2 + \varphi_{A,B}$	$\frac{\pi}{2} < \varphi_4 + \varphi_B - \varphi_2 < \frac{3\pi}{2}$
12	I_1	I_2	0	I_4	I_1	$\varphi_{1,2} + \varphi_{A,B}$	$\frac{\pi}{2} < \varphi_4 + \varphi_B - \varphi_{1,2} < \frac{3\pi}{2}$
13	0	0	I_3	I_4	I_3	$\varphi_{3,4} + \varphi_B$	-
14	I_1	0	I_3	I_4	I_1	$\varphi_{A,B}$	$\frac{\pi}{2} < \varphi_{3,4} + \varphi_B < \frac{3\pi}{2}$
15	0	I_2	I_3	I_4	I_2	$\varphi_2 + \varphi_{A,B}$	$\frac{\pi}{2} < \varphi_{3,4} + \varphi_B - \varphi_2 < \frac{3\pi}{2}$
16	I_1	I_2	I_3	I_4	I_1	$\varphi_{1,2} + \varphi_{A,B}$	$\frac{\pi}{2} < \varphi_{3,4} + \varphi_B - \varphi_{1,2} < \frac{3\pi}{2}$

These modifications must be inserted into Table I and Tables III and IV respectively.

Situation 8 is represented from a pulse $I_1 | \varphi_{1,2}$ that exits the first device and enters the input A second-level device, while a pulse $I_3 | 0$ exits the second device and enters the input B second-level device, where it propagates in the secondary input waveguides, emerging as $I_3 | \varphi_B$. The repulsion takes place if

$$\frac{\pi}{2} < \varphi_B - \varphi_{1,2} < \frac{3\pi}{2} \quad (33)$$

which generates $I_2 | \varphi_{1,2} + \varphi_{A,B}$ as output. To respect this phase condition, it is necessary to make a further restriction on $\varphi_{1,2}$ that is

$$0 < \varphi_{1,2} < \frac{\pi}{2}. \quad (34)$$

This modification must be inserted into Table I.

Situation 9 is represented from an absence of pulse from the exits of the first device and from a pulse $I_4 | \varphi_4$ that exits the second device and enters the input B second-level device, where it propagates in the secondary input waveguides, emerging as $I_4 | \varphi_4 + \varphi_B$.

Since this pulse reaches the output without interacting with other pulses, it is not necessary to impose any phase condition on the first-level devices.

Situation 10 is the most important for this connection since it denies the possibility of full cascading for this kind of device. It is represented from a pulse $I_1 | 0$ that exits the first device

and enters the input A second-level device, while a pulse $I_4 | \varphi_4$ exits the second device and enters the input B of the second-level device, where it propagates in the secondary input waveguides, emerging as $I_4 | \varphi_4 + \varphi_B$. The repulsion takes place, at the converging point, if

$$\frac{\pi}{2} < \varphi_4 + \varphi_B < \frac{3\pi}{2} \quad (35)$$

that would generate $I_1 | \varphi_{A,B}$ as output if (35) is satisfied. Unfortunately, this is not possible since we have to respect the phase condition $(\pi/2) < \varphi_4 < 3\pi/2$ expressed from Table II and the phase condition expressed from (32). This means that $\varphi_4 + \varphi_B > 3\pi/2$, denying (35).

The others input conditions are reported into Table IV just for completeness without any further discussion since this kind of cascade configuration is not able to work properly due to the restriction imposed from the phase conditions. We report them to show another inconvenience that would have anyway invalidated this configuration even if the phase condition were satisfied. If we look at the outputs, we see that we obtain equal exit pulses for the inputs labeled 6,10,14; 7,11,15; and 8,12,16 even if we are in the presence of different input configurations. This means that this kind of cascade is not able to code as a phase information all the possible input configurations. Due to the fact that the output pulses are equal not only in phase but even in intensity, it is not possible to avoid this output superposition using different intensified input pulses.

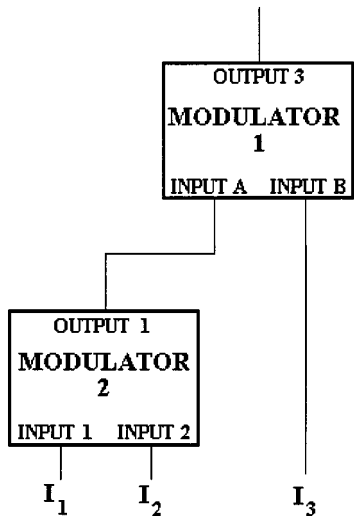


Fig. 7. Half-cascade of 1+1 devices.

We have seen until this point that it is impossible, for the device as it stands, to be connected in a full cascade configuration. If we further look at Table IV, we can see that the cascade is able to work properly for the first nine configurations with proper phase conditions. If we consider only the first nine input configurations, we see that they represent a half-cascade device, that is, a device composed from a first-level device with two inputs and a second-level device whose inputs are composed from the output of the first-level device and from direct input pulse streams. This half-cascade configuration is shown in Fig. 7. The operative scheme for this half-cascade configuration is shown in Tables V–VII. Because we use only three inputs, it is possible to speed the transmission velocity up to three times the velocity of input channels. Due to the direct entrance of flow 3 inside the second-level device with respect to flows 1 and 2 that are first speeded from the first-level device, it is necessary to delay flow 3 to synchronize it with the output of the first-level device.

The full cascade is probably possible if we use a different phase coding mechanism for the base device, but this is not in the scope of this paper. We wish to suggest first an example of a totally optical device capable to speed up the transmission velocity of an optical channel.

Further considerations about the temporal behavior and the absorbing behavior of solitons in transverse refractive index profile device have already been studied [13], [14] and are not repeated here for brevity.

VII. EXAMPLE OF DESIGN OF THE RECEIVER

We now design a proper demodulator device able to translate the phase information of the input channel into a binary information of two output channels. We use the same design criteria used for the modulator device because they allow a high degree of freedom. A simulation of this receiver device from the numerical point of view using an FD-BPM algorithm to verify the agreement with the theory is also presented.

We use as design criteria the features of the output pulses of the modulator reported in Section IV, which are $C = 20$ for the amplitude of the beam, $\beta = 30$ for the wavevector, a phase

value equal to zero when it is codified the presence of a pulse in the first input only, a phase value equal to 0.55π when it is codified the presence of a pulse in the second input only, and a phase value equal to 1.24π when it is codified the presence of the pulses in both inputs of the modulator.

Since we deal with phase information, it is necessary to assume the existence of a phase referring into the demodulator, which allows the extraction of the mentioned information from the received pulses. This is what normally happens in this kind of devices, where an internal clock signal is present that is properly synchronized with the incoming data flow using an initial sequence that is sent from the transmitter to the receiver before starting the data transmission. This operation allows the synchronizing of the clock of the receiver.

The structure of the demodulator is shown in Fig. 8, where it is possible to see that both the received pulses and the clock pulses enter into the device. Supposing that the clock pulses have already been synchronized with zero phase delay with respect to the received pulses, the clock input waveguide is calculated so that the clock pulses experience a relative phase variation equal to 2π : this is equal to say that there is not variation with respect to the input phase.

Each clock pulse propagates parallel and partially overlapped with each data pulse, interacting with it: the interaction acceleration is a cosinusoidal function of their relative phase ϕ and an exponential function of their relative distance d according to [18]

$$a(d, \phi) = \frac{C^2}{5} \exp(-C(d - 2x_{\text{HHHW}})) \cos \phi \quad (36)$$

with the condition ($d \geq 2x_{\text{HHHW}}$). x_{HHHW} is the half-height half-width that is the distance from the center of the beam where the amplitude reduces to one-half. It is possible to demonstrate that

$$x_{\text{HHHW}} = \frac{1}{C} \log(2 + \sqrt{3}) \quad (37)$$

which is a function of the amplitude C .

Because the interaction acceleration depends on the relative phase, the data pulse is repulsed toward the opposite side of the waveguide after a certain propagation distance that is a function of the relative phase: if in correspondence of each propagation distance related to a proper phase value an exit is placed, we obtain a proper demultiplexing device based on the phase of the incoming pulse.

The closer the relative phase is to π , the shorter the propagation distance is, because the data pulse is strongly repulsed. On the contrary, the closer the relative phase is to $\pi/2$, the longer the propagation distance is, because the data pulse is weakly repulsed.

To allow the repulsion between the clock beam and the data beam, a phase value equal to $3/2\pi$ should be chosen for the clock beam and a phase value included between 0 and π for the data beam. This would impose further restrictions on the phase modulation values that we want to avoid.

For this reason, a phase value equal to zero is chosen for the clock beam, implying that it is attracted by the zero phase data beam, merging together and generating a unique double amplitude output beam. This situation does not represent a problem

TABLE V
WORKING SCHEME OF THE FIRST DEVICE (FIRST-LEVEL DEVICE) WHOSE PHASE CONDITIONS ARE PROPERLY MODIFIED TO BE CONNECTED IN A HALF-CASCADE CONFIGURATION

N°.	INPUT 1 (INTENSITY)	INPUT 2 (INTENSITY)	OUTPUT INTENSITY	OUTPUT PHASE	PHASE CONDITION
1	0	0	0	0	-
2	I_1	0	I_1	0	-
3	0	I_2	I_2	φ_2	$\frac{\pi}{2} < \varphi_2 < \pi$
4	I_1	I_2	I_1	$\varphi_{1,2}$	$0 < \varphi_{1,2} < \frac{\pi}{2}$

TABLE VI
WORKING SCHEME OF THE THIRD DEVICE (SECOND-LEVEL DEVICE) WHOSE PHASE CONDITIONS ARE PROPERLY MODIFIED TO BE CONNECTED IN A HALF-CASCADE CONFIGURATION

N°.	INPUT A (INTENSITY)	INPUT B (INTENSITY)	OUTPUT INTENSITY	OUTPUT PHASE	PHASE CONDITION
1	0	0	0	0	-
2	I_A	0	I_A	0	-
3	0	I_B	I_B	φ_B	$\pi < \varphi_B < \frac{3}{2}\pi$
4	I_A	I_B	I_A	$\varphi_{1,2}$	-

TABLE VII
WORKING SCHEME OF THE HALF-CASCADE DEVICE. THE PHASE CONDITIONS ARE INCLUDED IN THE WORKING SCHEME OF THE DEVICES (TABLES V AND VI) THAT COMPOSE THE CONFIGURATION

N°.	INPUT 1 (INTENSITY)	INPUT 2 (INTENSITY)	INPUT 3 (INTENSITY)	OUTPUT INTENSITY	OUTPUT PHASE
1	0	0	0	0	0
2	I_1	0	0	I_1	0
3	0	I_2	0	I_2	φ_2
4	I_1	I_2	0	I_1	$\varphi_{1,2}$
5	0	0	I_3	I_3	φ_B
6	I_1	0	I_3	I_1	$\varphi_{A,B}$
7	0	I_2	I_3	I_2	$\varphi_2 + \varphi_{A,B}$
8	I_1	I_2	I_3	I_1	$\varphi_{1,2} + \varphi_{A,B}$

because the original amplitude can be recovered using a proper beam splitter at the output of the receiver related to the zero phase data beam.

For the modulation phase value chosen, it is possible to see from the receiver structure shown in Fig. 8 that the zero phase value merges together with the clock beam reaching output 1, which represents the output related to the first channel. The situation related to the presence of only one pulse on the second channel has been coded with a 0.55π phase value, which implies a weak repulsion and therefore a quite long propagation distance where it reaches output 2.

The situation related to the presence of pulses on both the channels has been coded with a 1.24π phase value, which implies a strong repulsion and therefore a short propagation distance where it reaches output waveguide 3. Because this output pulse must be used to generate two output pulses in channel 1

and 2 to recover the original signal, it is necessary to introduce a proper external beam splitter whose output beams are sent to channels 1 and 2 using proper optical connections. If it is necessary to recover the original amplitude, a proper optical amplifier that doubles the amplitude of the input beam before sending it to the beam splitter must be introduced.

The receiver is equipped with a clock drain waveguide that extracts the clock pulse after the interaction with the data pulse, except for the situation where the data pulse phase is equal to zero, which implies the merging between the two pulses.

This receiver also can be used for a three-channel modulator adding proper outputs in correspondence of the propagation distance related to the relative phase values.

We want now to show an example of the design of the receiver that is simulated by the numerical point of view, using as parameters the features of the pulses generated from the modulator.

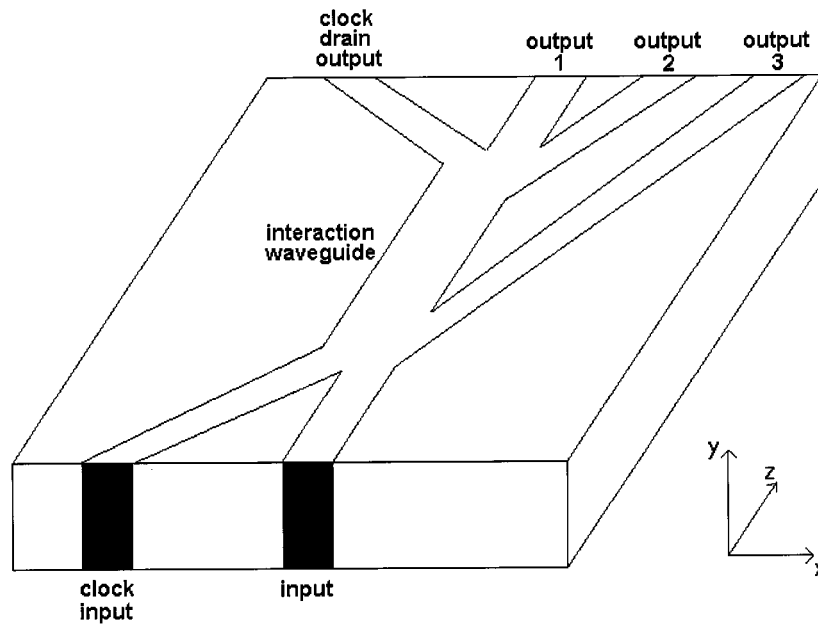


Fig. 8. 3-D view of the structure of the receiver.

It is first necessary to give more details about the interaction mechanism between solitons to derive an exact formula that allows calculation of the exit propagation distance as a function of the relative phase and of the other parameters of the receiver.

Due to the expression of (36), the interaction acceleration varies with the relative distance: this means that the repulsive action decreases during propagation while the relative distance increases. Because we are not interested in the exact trajectory followed by the soliton beams during the interaction but are interested in the distance that the beam has to propagate along the longitudinal axis to move transversally from the center to the lateral side of the waveguide, where the exits are placed, it is possible to use the mean acceleration along the transversal path [12] instead of the instantaneous acceleration expressed by (36). The mean acceleration is defined as

$$\bar{a} = \frac{1}{b} \int_0^b a(x) dx \quad (38)$$

where b is the transversal path. In this case, it is a negative quantity since it decreases when the beam moves from zero and it is necessary to use its modulus.

The total transversal acceleration a_M is composed by the difference between the modulus of acceleration expressed by (38) and the acceleration a_T generated by the index profile that is constant and is expressed by (2)

$$a_M = |\bar{a}| - a_T. \quad (39)$$

The equation that expresses the transverse distance x as a function of propagation coordinate z is

$$x = \frac{1}{2} a_M z^2. \quad (40)$$

We already said that we are interested to know z as a function of the transverse path $x = b$. Substituting $x = b$ in (40) and

solving with respect to z , excluding the nonphysical solution, we have

$$z_d = \left(\frac{2b}{a_M} \right)^{\frac{1}{2}}. \quad (41)$$

The relative distance d of (36) is composed by an initial interaction distance d_0 depending on the geometry of the waveguide and a variable distance x . Substituting (36) into (38), using $d = d_0 + x$, we have

$$\bar{a} = \frac{C \cos \varphi}{5b} \left(\exp(-C(b + d_0 - 2x_{HHHW})) - \exp(-C(d_0 - 2x_{HHHW})) \right). \quad (42)$$

Once derived, the relation, expressed by the (41), between the exit propagation distance and the relative phase between the clock beam and the data beam, it is possible to continue with the design of the receiver.

Because the width of the data beam is related to the amplitude C of the hyperbolic secant profile through (37), using the same criterion used for the modulator, we choose a waveguide characterized by a width $2b$ equal to 0.5.

If we choose the refractive index of the waveguide Δn_0 to be equal to $7.27 \cdot 10^{-5}$ and we fix the initial distance d_0 between the two beams to be equal to b , that is, the distance between the two parallel waveguides composing the interaction waveguide is equal to b , then substituting the numerical values into (41) using (39), (42), and (2), we obtain for the relative phase values 0.55π and 1.24π an exit propagation distance equal to 30 and one, respectively.

The left-hand side of the interaction waveguide is characterized by a quite higher refractive index with respect to the right-hand side to avoid that the clock pulse is moved from its initial position during the propagation due to the reciprocal repulsive action with respect to the data pulse.

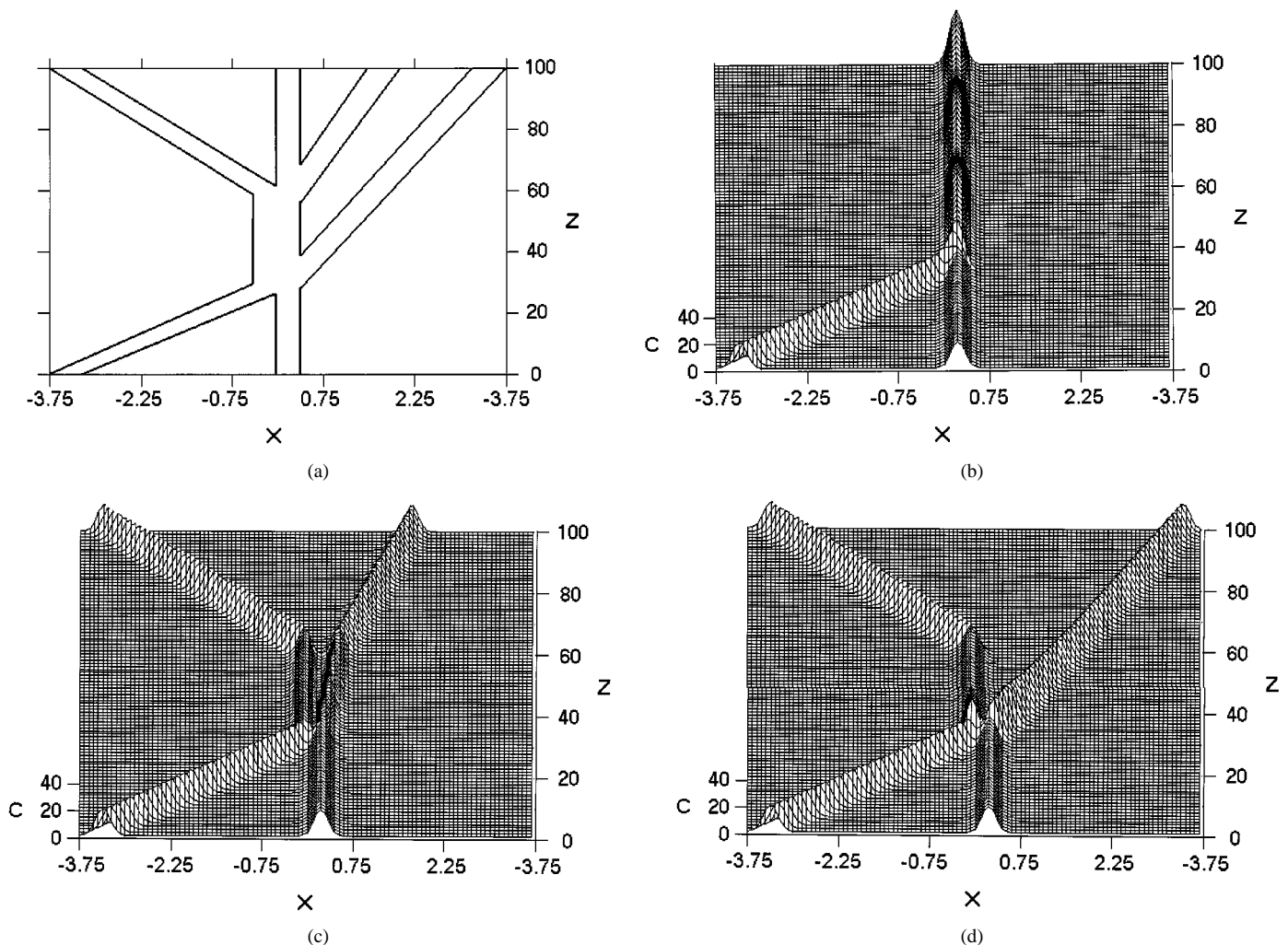


Fig. 9. (a) Upper view of the structure of the receiver. (b) Numerical simulation of the behavior of the receiver in the presence of the zero phase data pulse, corresponding to the presence of only one pulse in channel 1. The clock pulse and the data pulse merge together: the resulting pulse reaches the output 1. (c) Numerical simulation of the behavior of the receiver in the presence of the 0.55π phase data pulse, corresponding to the presence of only one pulse in channel 2. The clock pulse and the data pulse weakly repulse each other; the data pulse reaches output 2. (d) Numerical simulation of the behavior of the receiver in the presence of the 1.24π phase data pulse, corresponding to the presence of one pulse in both channels. The clock pulse and the data pulse strongly repulse each other: the data pulse reaches output 3.

Once the interaction waveguide is designed, it is necessary to design all the input–output optical structures to this main waveguide.

Since the clock beam must be in-phase with the zero phase value of the data pulse, it is necessary to design a clock input waveguide whose difference of optical path with the input waveguide is a multiple of 2π . If we choose the waveguide shown in Fig. 9(a), characterized by the same refractive index of the interaction waveguide, it is immediate possible to verify that it respects this condition and the paraxial condition, and that its lock-in threshold is low enough to trap the beams whose amplitude C is equal to or greater than 20, as the ones we are using.

At the end of the interaction waveguide, on the left side, the clock drain waveguide is placed that is necessary to extract the clock pulses after the interaction with the data pulses. Its refractive index Δn_0 has been chosen to be equal to $1 \cdot 10^{-4}$ that is a bit higher value with respect to the interaction waveguide to guarantee the data pulse to reach the input of this waveguide, except in the situation of attraction and merging with the data pulse.

It is immediately possible to verify that the chosen clock drain waveguide respects the paraxial approximation and has a proper lock-in threshold.

On the right side of the interaction waveguide are placed the output waveguides that allow the exit of the data pulses, which are repulsed from the clock pulses. Their geometry has been designed to respects the paraxial approximation and have a proper lock-in threshold.

The geometry of the designed receiver is shown in Fig. 9(a). Let us analyze the results of the numerical simulations for the three possible input combinations to demonstrate the correctness of the developed theory, neglecting the situation of no inputs that represents the first combination according to Table I.

In Fig. 9(b), the numerical simulation of the receiver in the case of the presence zero phase input pulse at the input (the second input combination of Table I) is shown. In this situation, since the relative phase difference between the data pulse and the clock pulse is equal to zero, an attractive acceleration results, according to the (36), and the two beams collapse, reaching output 1.

In Fig. 9(c), the numerical simulation of the receiver in the case of the presence of 0.55π phase input pulse at the input (the third input combination of Table I) is shown. In this situation, because the relative phase difference between the data pulse and the clock pulse is equal to 0.55π , a weak repulsive acceleration results, according to (36), and the data pulse is pushed toward the right-hand side after a certain propagation distance, reaching output 2.

In Fig. 9(d), the numerical simulation of the receiver in the case of the presence of 1.24π phase input pulse at the input (the fourth input combination of Table I) is shown. In this situation, since the relative phase difference between the data pulse and the clock pulse is equal to 1.24π , a strong repulsive acceleration results, according to (36), and the data pulse is pushed toward the right-hand side after a very short propagation distance, reaching output 3.

The numerical simulations, as shown in Fig. 9, confirm the correctness of the developed receiver.

VIII. CONCLUSION

We have studied and designed an all-optical modulator device, whose working principles are based on the repulsive and propagation properties of solitons in a parabolic transverse refractive index profile, which we analyzed in this paper.

The switching properties have been studied in detail, obtaining some useful design criteria for a practical device. The device can be properly designed by means of the geometrical and optical parameters of the different structures that compose the modulator.

It has been demonstrated that the device, as it stands, can be connected in a half-cascade configuration, capable of accepting three input streams of pulses and generating a unique stream of pulses whose information capacity is three times greater than the capacity of input streams.

A proper demodulator device has also been designed and simulated to work in couple with the proposed modulator.

The whole system can be considered as a complement to and an improvement of the wavelength-division multiplexing (WDM) technology since it allows one to increase the transmission capacity of each binary channel at its given wavelength. Using a number of modulator systems equal to the number of the wavelength channels, the total capacity of the WDM system is increased.

REFERENCES

- [1] R. Y. Cio, E. Garmire, and C. H. Townes, "Self-trapping of optical beams," *Phys. Rev. Lett.*, vol. 13, pp. 479–482, 1964.
- [2] B. Luther-Davies and Y. Xiaoping, "Waveguides and Y junctions formed in self-defocusing dark spatial soliton," *Opt. Lett.*, vol. 17, pp. 496–498, 1992.
- [3] W. Krolikowski and Y. S. Kivshar, "Soliton-based optical switching in waveguide arrays," *J. Opt. Soc. Amer. B*, vol. 13, pp. 876–887, 1996.
- [4] N. N. Akhmediev and A. Ankiewicz, "Spatial soliton X-junctions and couplers," *Opt. Commun.*, vol. 100, pp. 186–192, 1993.
- [5] W. Krolikowski, X. Yang, B. Luther-Davies, and J. Breslin, "Dark soliton steering in a saturable nonlinear medium," *Opt. Commun.*, vol. 105, pp. 219–225, 1994.
- [6] A. P. Sheppard, "Devices written by colliding spatial solitons: A coupled mode theory approach," *Opt. Commun.*, vol. 102, pp. 317–323, 1993.
- [7] J. P. Gordon, "Interaction forces among solitons in optical fibers," *Opt. Lett.*, vol. 8, pp. 596–598, 1983.

- [8] F. Garzia, C. Sibilila, M. Bertolotti, R. Horak, and J. Bajer, "Phase properties of a two-soliton system in a non linear planar waveguide," *Opt. Commun.*, vol. 108, pp. 47–54, 1994.
- [9] A. B. Aceves, J. V. Moloney, and A. C. Newell, "Reflection and transmission of self-focused channels at nonlinear dielectric interfaces," *Opt. Lett.*, vol. 13, pp. 1002–1004, 1988.
- [10] P. Varatharajah, A. B. Aceves, and J. V. Moloney, "All-optical spatial scanner," *App. Phys. Lett.*, vol. 54, pp. 2631–2633, 1989.
- [11] A. B. Aceves, P. Varatharajah, A. C. Newell, E. M. Wright, G. I. Stegman, D. R. Heatley, J. V. Moloney, and H. Adachihara, "Particle aspects of collimated light channel propagation at nonlinear interfaces and in waveguides," *J. Opt. Soc. Amer. B*, vol. 7, pp. 963–974, 1990.
- [12] F. Garzia, C. Sibilila, and M. Bertolotti, "Swing effect of spatial soliton," *Opt. Commun.*, vol. 139, pp. 193–198, 1997.
- [13] ———, "High pass soliton filter," *Opt. Commun.*, vol. 152, pp. 153–160, 1998.
- [14] ———, "All optical soliton based router," *Opt. Commun.*, vol. 168/1–4, pp. 277–285, 1999.
- [15] H. W. Chen and T. Liu, "Nonlinear wave and soliton propagation in media with arbitrary inhomogeneities," *Phys. Fluids*, vol. 21, pp. 377–380, 1978.
- [16] P. K. Cow, N. L. Tsintsadze, and D. D. Tsakhaya, "Emission of ion-sound waves by a Langmuir soliton moving with acceleration," *Sov. Phys.-JETP*, vol. 55, pp. 839–843, 1982.
- [17] J. S. Aitchison, A. M. Weiner, Y. Silberberg, M. K. Oliver, J. L. Jackel, D. E. Leaird, E. M. Vogel, and P. W. E. Smith, "Observation of spatial optical solitons in a nonlinear glass waveguide," *Opt. Lett.*, vol. 15, pp. 471–473, 1990.
- [18] F. Garzia, C. Sibilila, and M. Bertolotti, "All optical serial switcher," *Opt. Quantum Electron.*, vol. 32, pp. 781–798, 2000.
- [19] B. Luther-Davies and Y. Xiaoping, "Steerable optical waveguides formed in self-defocusing media by using dark spatial soliton," *Opt. Lett.*, vol. 17, pp. 1755–1757, 1992.

Fabio Garzia received the degree in electronics engineering and the Ph.D. degree in applied electromagnetism from the University "La Sapienza," Rome, Italy, in 1992 and 1997, respectively.

Since 1997, he has been a Lecturer of applied security, physics, optics, and quantum electronics arguments with the Faculty of Engineering, University "La Sapienza." Since 1999, he has been Head of the Applied Security Laboratory, Dipartimento di Energetica, INFN, of the same university. His research interests are all-optical devices, image processing, biometrics and pattern recognition for applied security applications, telecommunications, and optical computing. He is the author of numerous papers in international journals.

Concetta Sibilila (M'97) received the degree in physics from the University "La Sapienza," Rome, Italy, in 1976.

From 1981 to 1986, she was an Assistant Professor in general physics with the Faculty of Engineering of the same university. Since 1986, she has been an Associate Professor in physics there. She worked on quantum aspects of nonlinear optics. Her current research interests are in quasi-periodical structures and application of nonlinear optics to new filters. Part of her research activity is devoted to the study of materials and in particular to thermophysical properties of materials. She is the author of more than 100 papers on international journals.

Prof. Sibilila is a member of the Optical Physical Society, the European Physical Society, and the Optical Society of America (OSA).

Mario Bertolotti is a full Professor of physics at the Faculty of Engineering, University "La Sapienza," Rome, Italy. He is interested in lasers and their properties and applications, carrying out studies on coherence, propagation in atmosphere, scattering, and holography, and on several devices and applications including laser annealing, and liquid crystal modulators. Recently, he has become interested in integrated optics and, in particular, propagation in nonlinear guides. He is the author of many scientific publications in several international journals and books.

Prof. Bertolotti is a member of the Optical Society of America (OSA).